Spatial pattern of the green heat sink using patch- and network-based analysis: implication for urban temperature alleviation

Zahra Mokhtari, Shahindokht Barghjelveh*, Romina Sayahnia, Peyman Karami, Salman Qureshi, Alessio Russo

Zahra Mokhtari, PhD Candidate, Department of Environmental Planning and Design, Environmental Sciences Research Institute, Shahid Beheshti University, 1983969411 Tehran, Iran, Email: z_mokhtari@sbu.ac.ir

Shahindokht Barghjelveh*, PhD. (Corresponding author) Associate Professor, Department of Environmental Planning and Design, Environmental Sciences Research Institute, Shahid Beheshti University, 1983969411 Tehran, Iran, Email: s-barghjelveh@sbu.ac.ir

Romina Sayahnia, PhD. Assistant Professor, Department of Environmental Planning and Design, Environmental Sciences Research Institute, Shahid Beheshti University, 1983969411 Tehran, Iran, Email: r_sayahnia@sbu.ac.ir

Peyman Karami, PhD. Department of Environmental Sciences, Malayer University, Malayer, Iran, Email: peymankarami1988@gmail.com

Salman Qureshi, PhD. Senior Scientist, Department of Geography, Humboldt University of Berlin, Rudower Chaussee 16, Berlin 12557, Germany. Email: salman.qureshi@geo.hu-berlin.de

Alessio Russo, PhD. Senior Lecturer, School of Arts, University of Gloucestershire, Francis Close Hall Campus, Swindon Road, Cheltenham GL50 4AZ United Kingdom. Email: arusso@glos.ac.uk

Highlight

- Extracting the UGS from NDVI and LST using the diagnostic-ROC test.
- Providing cold green patches map using Getis Ord Gi* statistic.
- Proposing a framework to construct the green heat sink (GHS) network.
- Investigating the overall connectivity of GHS from a circuit theory perspective.
- Identifying the priority locations to improve the urban thermal environment.

Despite the evidence on the cooling effects of urban green spaces (UGS), little is known about how they function as an interconnected network of cold green patches or a green heat sink (GHS) within an urban landscape. This study aimed to analyze the general spatial pattern and connectivity of GHSs using the pertinent indices and Circuitcape tool in an Iranian urban area between 2000 and 2020. Initially, normalized differentiation vegetation index (NDVI) and land surface temperature (LST) maps were derived. To construct a network, GHS was extracted by Getis Ord Gi* statistic and the cost map was built by reversing the NDVI. The results showed that UGS and GHSs shrunk by 17% and 31%, respectively, and became highly fragmented, demonstrating smaller sizes while the number of patches, patch density, and the complexity of the shape increased. According to the network analysis, the overall connectivity of GHSs decreased over time in 2020. Finally, five high-priority locations were identified to increase the connectedness of vegetation cover that might improve the thermal environment of the city. This research can direct urban planning towards enhancing a green space network to mitigate the urban temperature within the urban landscape.

Keywords: Functional connectivity; Climate regulation service; Local spatial statistic; Circuit theory; Landscape planning; Karaj City.

1. Introduction

Urban ecosystems are characterized by a heterogeneous mosaic of different natural and anthropogenic land uses (Darvishi et al., 2020; Peng et al., 2016; Qureshi et al., 2014) with a highly modified surface-atmosphere energy balance and thermal environment (Voogt & Oke, 2003; Weng, 2009). Hence, urban areas exhibit unique thermal environments that are warmer than surrounding rural areas, which is known as Urban Heat Island (UHI) (Voogt & Oke, 2003). Our current knowledge of the urban thermal environment (UTE) is principally based on retrieving land surface temperature (LST) from satellite thermal sensors (Bokaie, Zarkesh, Arasteh, & Hosseini, 2016; Peng et al., 2016). In cities, the urban green space (UGS) function can contribute to mitigating high temperatures (Masoudi et al., 2021; Zardo et al., 2017) and improving the UTE through coping with climate change effects (Reis & Lopes, 2019; Saaroni et al., 2018). While urbanization growth alters the quantity and quality of UGS (Masoudi et al., 2021) and exacerbates the UHI effect (Du et al., 2020; Halder et al., 2021; Zhou & WANG, 2011; Pierik et al., 2016).

In an urban landscape, every single patch can be categorized as a heat source or heat sink (A. Chen et al., 2016; L. Chen, Fu, & Zhao, 2008; Li, Cao, Lang, & Wu, 2017; Zhao, Zhang, Miao, Ye, & Min, 2018); which are almost identified based on land use/land cover (LULC) classes (Pramanik & Punia, 2020). The urban green space (UGS) is known as the best-performing heat sink in urban areas (Li, Cao, Lang, & Wu, 2017). UGS refers to any type of vegetation cover from forests, bushland, and parks to agricultural land that provides multiple ecosystem services (Bastian, Haase, & Grunewald, 2012; L. Taylor & Hochuli, 2017) such as cooling effect service (Zardo et al., 2017). Drawing from landscape ecology science, indicating that patterns affect ecological processes and functions (Turner, et al., 1989), recent studies have shown that the functionality of UGSs related to the cooling service is highly dependent upon their spatial pattern within the urban landscape (Masoudi & Tan, 2019). The spatial pattern of UGS can be

delineated by the spatial distribution and their geometric characteristics, generally described by compositional (i.e., patch abundance) and configurational (i.e., arrangement like connectivity and fragmentation) attributes (McGarigal & Marks, 1995). This pattern-function association has been well investigated concerning the cooling impacts of UGSs (Bao, Li, Zhang, Zhang, & Tian, 2016; Connors, Galletti, & Chow, 2013; Li et al., 2017; Maimaitiyiming et al., 2014; Sun, Xie, & Chen, 2018). Then, recently, optimizing UGS spatial patterns (e.g., the distance between green patches) to intensify the cooling effect gained attention in urban planning (Masoudi & Tan, 2019; Shih, 2017; Lin, Yu, Chang, Wu, & Zhang, 2015).

Connectivity of UGS is one of the main principles used to address the landscape pattern-function association that often plays an essential role in high-temperature regulation (Xie et al., 2015; Zhang, Meerow, Newell, & Lindquist, 2019; Zhibin, Haifeng, Xingyuan, Dan, & Xingyang, 2015). The connectivity can be defined in two ways: structural and functional or potential connectivity. The former can be measured by spatial indices (Calabrese & Fagan, 2004). Functional connectivity refers to a degree of facilitating or impeding movements of species or the flow of energy, materials, and nutrients among patches (Darvishi et al., 2020; Leitão, Miller, Ahern, & McGarigal, 2012; Marulli & Mallarach, 2005; P. D. Taylor, Fahrig, Henein, & Merriam, 1993). Implying the structural connectivity concept by landscape metrics in urban environments, a large number of studies revealed that the performance of green patches in lowering the urban temperature (i.e., cooling potential) reduces in poorly connected UGSs. For instance, Asgarian et al. (2015) used landscape spatial metrics (i.e., patch-based analysis) to measure the connectivity of UGS in Isfahan, central Iran. They found that the cooling effect of UGS decreases with increasing distance to other UGS and reducing UGS size and spatial geometry. Xie et al. (2015) explored the connectivity of the UGS and its relationship with temperature using morphological metrics and found that their connectedness contributes to improving the UTE. Kowe et al. (2021) examined the impact of the spatial configuration of vegetation patches on UTE, revealing that clustered and connected vegetation patches are more effective in alleviating urban surface temperature.

In addition to the patch-based analysis that measures the proximity and connectivity between patches (the above-mentioned studies), the network-based approach can model and evaluate the overall connectivity across an entire landscape (Urban, Minor, Treml, & Schick, 2009; Grafius, Corstanje, Siriwardena, Plummer, & Harris, 2017; Kong, Yin, Nakagoshi, & Zong, 2010). In other words, the network approach can quantify both structural and functional connectivity and can evaluate the function of a landscape. Simply, a network is a set of nodes (or ecological sources or source patches) connected by links (Lookingbill & Minor, 2017). Among the available models to analyze the connectivity, circuit theory, which originated from electrical studies, offers an approach to investigating optimal least-cost pathways between landscape nodes (McRae, Dickson, Keitt, & Shah, 2008). This model uses resistance raster maps relevant to measure the degree of connectivity between landscape nodes (Koen, Bowman, Sadowski, & Walpole, 2014; Pelletier et al., 2014). In urban landscapes, the network has been used to enhance connectivity and optimize the green network planning associated with ecological purposes (Liu, Huang, & Zheng, 2022; Cui et al., 2020; Hyseni et al., 2021; Kwon, Kim, & Ra, 2021; Grafius et al., 2017; Uy & Nakagoshi, 2007; Guo, Saito, Yin, & Su, 2018; Zhang et al., 2019). For instance, Liu et al. (2022) extracted green patches to construct a green network to improve connectivity and determine the priority conservation areas in Beijing, China. They concluded that Circuit theory can optimize the UGS networks. However, the investigation of the UTE from a network- based perspective has seldom been reported in the scientific literature (Yu, Zhang, & Yang, 2021). Related to analyzing heat flow, Yu and colleagues (2021) defined a binary thermal landscape consisting of surface UHI patches and non-UHI areas. They applied Circuit theory to construct an LST-based UHI network to analyze the heat diffusion and consequently identify the critical locations to implement cooling measures in urban design and planning. As far as our best knowledge, despite the importance of UGS connectivity on cooling effect function, there is a lack of research to analyze the cold green patches or a green heat sink (GHS) connectivity and their cool airflow from the network-based perspective within an urban landscape.

Considering the above background, the main objective of the study is to investigate the effect of urbanization on dynamic spatial patterns (i.e., fragmentation) and overall connectivity of cold green patches or green heat sinks (GHS) using patch- and network-based approaches in a rapidly growing urban area in the north of Iran, between 2000 and 2020. The research framework would finally identify areas having a poor structural connection with thermal sinks and whose vegetation improvement will strengthen the cooling capacity of the study landscape to achieve a more thermally-comfort sustainable city. Generally, the current research was devised by answering the following questions: 1- how has the spatial pattern and overall connectivity of GHS changed during the past two decades due to the urbanization in Karaj city, 2- how we can propose an approach to identify the key elements in order to construct a GHS network using Circuitcape tool, 3- how the network analysis can help restore the GHS connectivity and consequently intensify the cooling effect.

2. Methodology

2.1. Study area

Karaj is the fourth most populated city in Iran located 36 km west of the capital Tehran, in the North of Iran. It has a total area of 220 km^2 spanning between 51° 0′ 30 E Longitude and 35° 48′ 45 N Latitude (Fig. 1). Historically, Karaj was regarded as a "garden city" with vast green areas. As is indicated in Fig. 1, due to intense urbanization (about a 30% increase in the built-up area) in the last twenty years, the gardens were gradually destroyed and replaced with residential areas. Vegetation cover in the study area includes gardens, municipal green areas, parks, agricultural lands, and dense and sparse rangelands (Mokhtari, Barghjelveh, & Sayahnia, 2021)**.** Karaj has followed a significant sprawl and scattered pattern of development expansion (Ghobadi, Khosravi, & Tavousi, 2018; Taleshi & Ghobadi, 2012), leaving plenty of vacant and barren land within the urban environment (Fig. 1). Currently, the city hosts a population of over 1,592,000 people (https://www.amar.org.ir). The region is characterized by an arid and semi-arid climate, according to De Martonne's climatic classification scheme, with hot summers and cold winters. July and February, with an average temperature of 34.6 and 9.2 °C, are the warmest and coldest months of the year, respectively (https://alborz.mporg.ir).

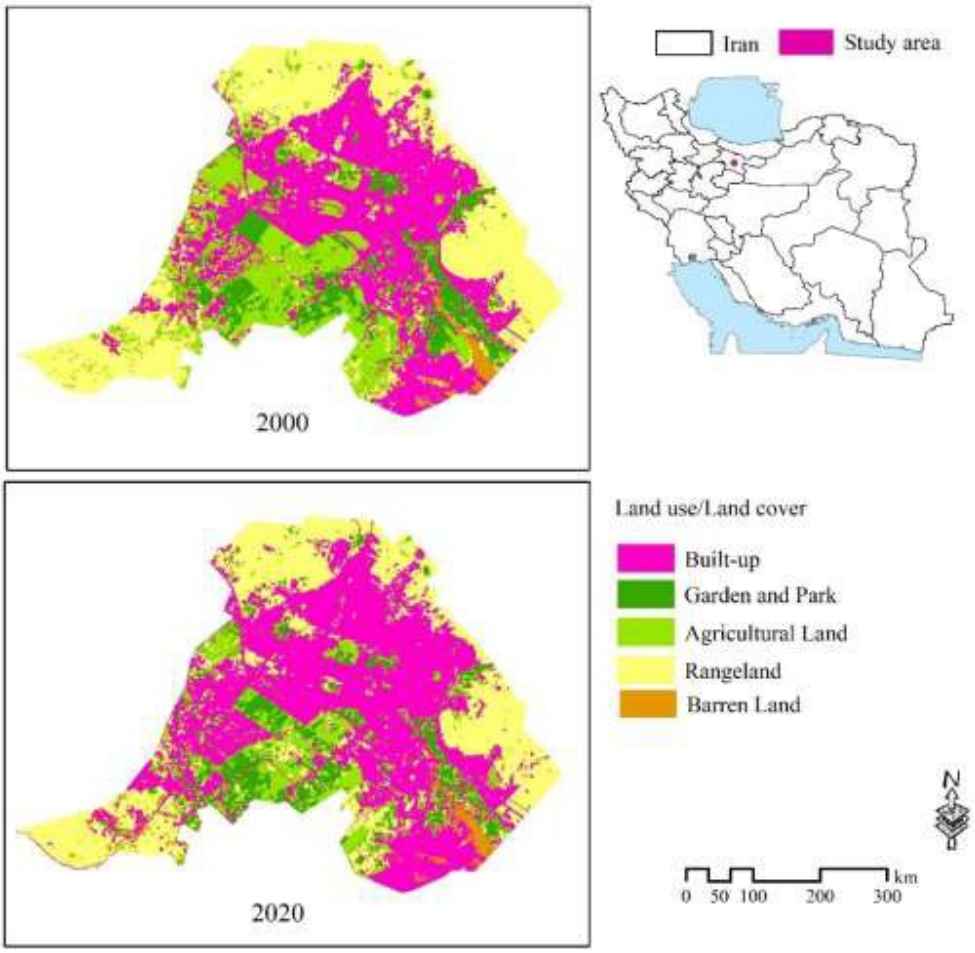

Fig. 1. Land use/ land cover map of Karaj city in 2000 and 2020

2.2. Data sources and pre-processing

Two cloud-free Landsat images taken on July 8, 2020 (Landsat 8 OLI-TIRS) and on July 17, 2000 (Landsat 7 ETM+) were acquired from the United States Geological Survey (USGS) website. Due to a lack of access to suitable images on the same day for both years, the closest dates in the given years were chosen. The images were selected in July, the hottest month in the region since the cooling effect of green space is important in this month. According to the meteorological data, the air temperature was 36°C, and no rain was reported in the last 24 hours in the acquisition days of two years.

2.3. Provision of NDVI and LST maps

The NDVI raster images for 2000 and 2020 were generated using the visible (RED) and near- infrared (NIR) reflectance bands of Landsat ETM+ and TRIS image data. This index ranges from -1 to +1 and has a positive relationship with vegetation biomass and abundance (Gillespie et al., 2018).

LST maps were retrieved using the Mono-Window (MW) algorithm (Qin, Karnieli, & Berliner, 2001; Wang et al., 2015). This algorithm applies one thermal infrared band (band 10 of OLI sensor and band 6 of ETM with 30 and 60-meter resolution, respectively). To retrieve LST maps, atmospheric transmittance and the effective mean atmospheric

temperature data were obtained from the meteorological database of the region. Digital numbers were first converted to spectral radiance using the gain and offset data provided in the image's metadata file in TXT format. The spectral radiance was then converted to at-satellite brightness temperature using satellite- and band-specific thermal conversion constants (known as K1 and K2). Finally, the land surface emissivity was applied to convert the at-satellite brightness temperature to land surface temperature. To do so, an NDVI-based technique proposed by Sobrino et al. (2008) was used to measure the surface emissivity by land use (soil and vegetation). Additional information regarding LST retrieval from Landsat images using the MW algorithm can be found in Qin et al., 2010 and Wang et al., 2015.

2.4. Extraction of UGS using optimal thresholding

Given the importance of UGS identification, it was necessary to provide a highly accurate UGS map. To do so, 300 training points were collected from vegetation cover of parks, gardens, and agricultural lands, and 300 samples were surveyed from the built-up area and barren land using an array of Landsat false-color composites and google earth images. Then the value of LST and NDVI was joined to the sample points for two years. Since NDVI and LST values vary with surface cover in urban landscapes (Bartesaghi-Koc, Osmond, & Peters, 2020), both maps were assumed to be able to determine the UGS. A diagnosis test (Labrique & Pan, 2010; Wong & Lim, 2011) was applied to identify the threshold value of each variable (i.e., NDVI and LST). In this research, the threshold value is a value of the variables that can diagnose the occurrence of a phenomenon (i.e., the presence of UGS). In the diagnosis test, the receiver operating characteristic (ROC) (Fawcett, 2006; Fluss, Faraggi, & Reiser, 2005) was used to analyze the ability of input variables in distinguishing UGS from non-UGS. Then, in the ROC curve, the optimal NDVI and LST thresholds were calculated using true skill statistics or the Youden's index (Fluss et al., 2005; Piri Sahragard, Ajorlo, & Karami, 2018) embedded in the ROCR package in R.3.5.2 and MedCalc version 13. The Youden index is a measure of the ROC curve, calculating the ability of a variable in distinguishing the sample points and also identifying the optimal threshold value (i.e., cut-off point) of the variable (Fluss et al., 2005).

In ROC, the area under the curve (AUC) has a range of values, varying from 0.5 to 1.0 (poor to perfect performance). In addition, the performance of each variable in distinguishing green areas can be evaluated using the Sensitivity, Specificity, Correct classification, and Miss classification criteria. Further description of ROC and various evaluation criteria, can be found in the following articles (Fawcett, 2006; Karami, Rezaei, Shadloo, & Naderi, 2020; Somodi, Lepesi, & Botta-Dukát, 2017).

2.5. Identification of GHSs

Since green patches extracted by thresholding of NDVI were thermally heterogeneous, to identify the significant green cold spots or green heat sinks, we used the Hot Spot Analysis tool available in the ArcGIS ESRI environment. This tool measures the Getis-Ord Gi* statistic, which is an intensity degree of spatial clustering for each spatial unit relative to its neighbors. The Gi* value is positive in areas with a cluster of high-intensity values and vice versa. The Gi* statistic calculation for a feature converts to a z-score (Jamei, Rajagopalan, & Sun, 2019). Moreover, p- value indicates probability in spatial pattern analysis: for instance, small p-values show low probabilities. So, the local statistics count on the tests for each location in the data and have two main identification purposes: local clusters and their significance (Caldas de Castro & Singer, 2006). Table 1 represents the critical p-values and z-scores for different confidence levels. For a statistically significant positive z-score, larger values imply a more intense cluster of high values (hot spot) while negative smaller values show the clustering of low values (cold spot) (Jana & Sar, 2016; Koen et al., 2014; Songchitruksa & Zeng, 2010). In this research, the LST map was analyzed using the z-score classification, with results varying from statistically significant negative to statistically significant positive at the different confidence levels of 99%, 95%, 90%, and not significant. Areas of high temperatures were identified as significant hot spots, whereas the areas with low temperatures were identified as significant cold spots. The cold spots included all kinds of classes like cold built-up and cold green areas. Considering the objective of this research, we analyzed only cold green patches at a 99% confidence level that was referred to as green heat sink (GHS).

Table 1 Classification of z-score and p-value in Hot Spot analysis (Arc GIS Desktop)

z-score(standard deviation)	p-value(Probability)	Confidence level
< -1.65 or > + 1.66	< 0. 10	90%
< -1.96 or > + 1.96	< 0.05	95%
< -2.58 or > + 2.58	< 0.01	99%

2.6. Construction of the network of GHSs

A network consists of a resistance map and user-defined nodes, which represent the core area in a landscape, and the resistance value is the opposite of the current or flow and is the inverse of the suitability of the flow or movement across the cells (or nodes) (McRae et al., 2008). In other words, an ost (or resistance) surface map is used to measure the degree of flow or movement between locations (Koen et al., 2014; Pelletier et al., 2014). In UTE studies, a resistance map must reflect the horizontal resistance to thermal diffusion or thermal flow (Yu et al., 2021). Studies in this field used different raster layers as cost maps**.** For instance, Yu et al (2021) used a land cover map to focus on the UHI network, assuming that the value of resistance in urban landscapes is related to the distance between different UHI patches. In other words, the resistance map is the inverse of a suitability map and is generated by the user considering the surface potential or effectiveness in impeding or facilitating the target flow (Grafius et al., 2017). The present research deals with the connectivity of the GHS network. Due to a lack of experimental knowledge related to weighing the role of different surfaces in cool airflow, we created the resistance map based on the NDVI map. Moreover, the NDVI map represents a measure of surface reflectance and is a critical indicator of land use/land cover identification (da Silva et al., 2020; Yengoh, Dent, Olsson, Tengberg, & Tucker III, 2015).

Then, To prepare the resistance layer, NDVI values were multiplied by minus one so that high vegetated areas present lower resistance to the connectivity of GHS and vice versa. The model result was finally evaluated to identify the strength of all possible pathways among the nodes of the landscape. In the literature on network analysis, pinch points are located in a specific area with a strong current flow (B. McRae et al., 2013; B. H. McRae et al., 2008); removing them can affect the connectivity of the network (Yu et al., 2021). So in this research, enhancing the vegetation cover in the pinch points significantly increases the overall connectivity of GHS. Commonly, these points can be identified visually based on the current density changes across a landscape (Pelletier et al., 2014). Identification of pinch point areas is advantageous in optimization planning and design of an urban landscape to mitigate temperature (Yu et al., 2021).

2.7. Patch-based analysis of GHS

The spatial pattern of GHSs was analyzed using a set of landscape metrics to understand the overall spatial pattern and fragmentation of GHSs in 2000 and 2020 using FAGSTATS 4.3 software. Drawing from the existing literature (Estoque, Murayama, & Myint, 2017; Liu, He, & Wu, 2016; Masoudi & Tan, 2019), the selected landscape metrics were percentage of landscape **(**PLAND), the number of patches (NP), patch density (PD), largest patch index (LPI), largest shape index (LSI) (McGarigal, 2015). Temporal changes in the spatial pattern of GHSs were interpreted to investigate the dynamics of the GHS network of the region. Table 2 shows a brief description of the selected landscape metrics. Figure 2 outlines the steps undertaken in the present research.

Table 2 Landscape metrics employed to analyze the spatial pattern (i.e., fragmentation) of GHS (McGarigal, 2015)

Landscape metric	Abbreviation	Description	Unit
Percentage of landscape	PLAND	Proportional abundance of a special patch type	Percentage
Number of patches	NP	Number of a special patch type in the landscape	None
Patch Density	PD	Number of special patches per unit area.	Number per 100 hectares
Largest patch index	LPI	The largest patch of a special patch type divided by total landscape area	None
Landscape shape index	LSI	A measure of the overall shape complexity of a special type of patches	None

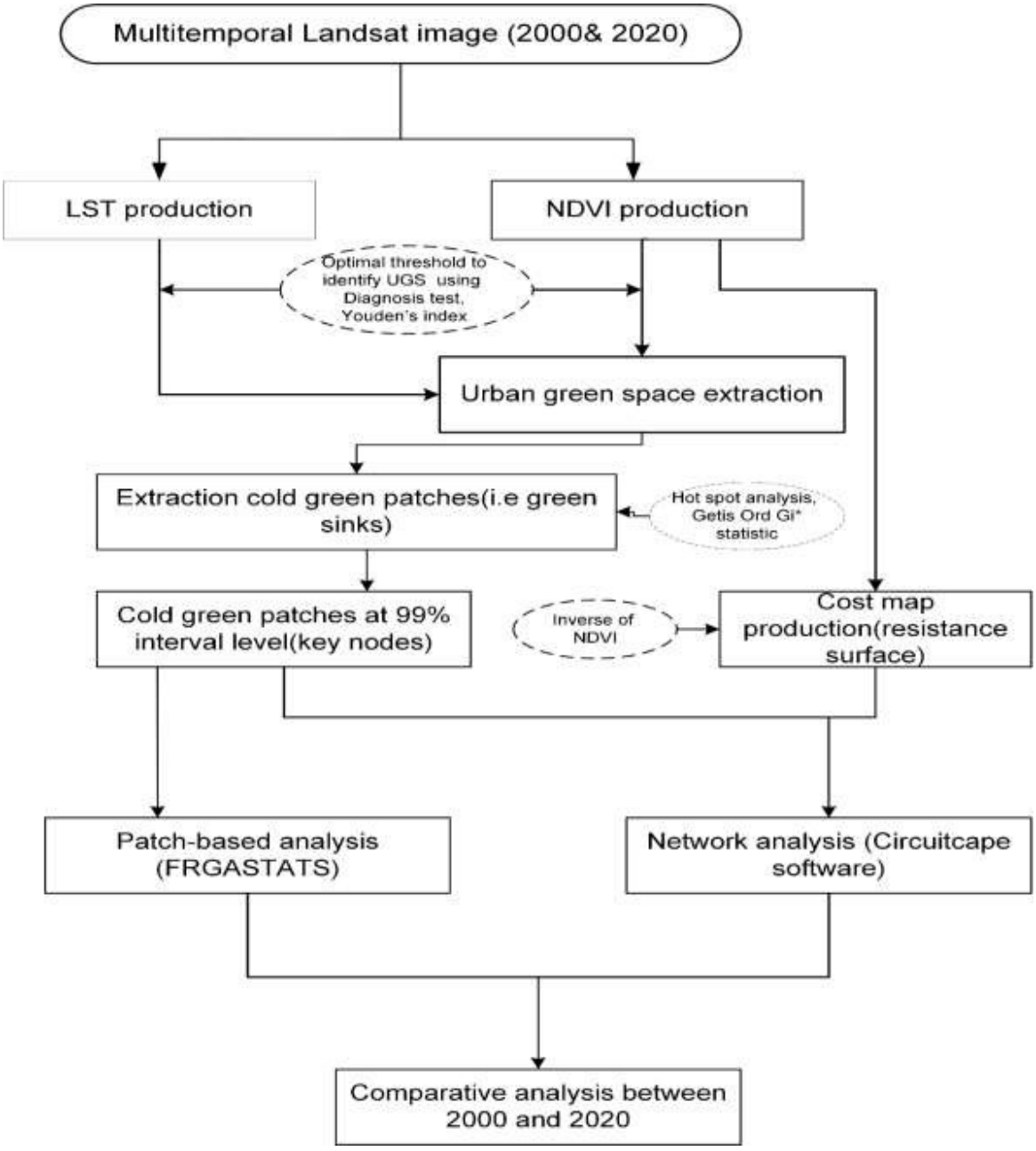

Fig. 2. Flowchart of the research methodology

3. Results

3.1. Results of the diagnostic-ROC test using NDVI and LST to extract UGS

The maps of NDVI and LST were provided to extract the UGS and GHS. Related to NDVI, minimum and maximum values were 0.79 ± 0.42 in 2000 and 0.82 ± 0.31 in 2020 (Fig. 3). Inspecting the google earth image and land use maps, the gardens, and some public parks, mainly in the south of the city has the highest NDVI (Fig.1). Minimum and maximum LST values were 28.5 and 56° C in 2000 and 31 and 57° C in 2020. LST values in Fig. 3 were distributed unevenly across the region in both years due to the high heterogeneity of land use/land cover classes (Fig. 1), so various types of vegetation cover, from sparse rangeland to dense gardens, substantially affected the LST. Observation showed that the barren land and poor rangeland had the highest temperature while the densely built-up area and gardens had the lowest LST. Comparing the LST maps indicated that in 2000 the UGS was the coldest, while in 2020, some vegetation cover lost its cooling effect (due to losing its quality), and the densely built-up area, mostly in the North and Central parts of the city, showed low LST. Generally, the reason for this phenomenon is rooted in the arid and semi-arid climatic zone of the region (see the discussion).

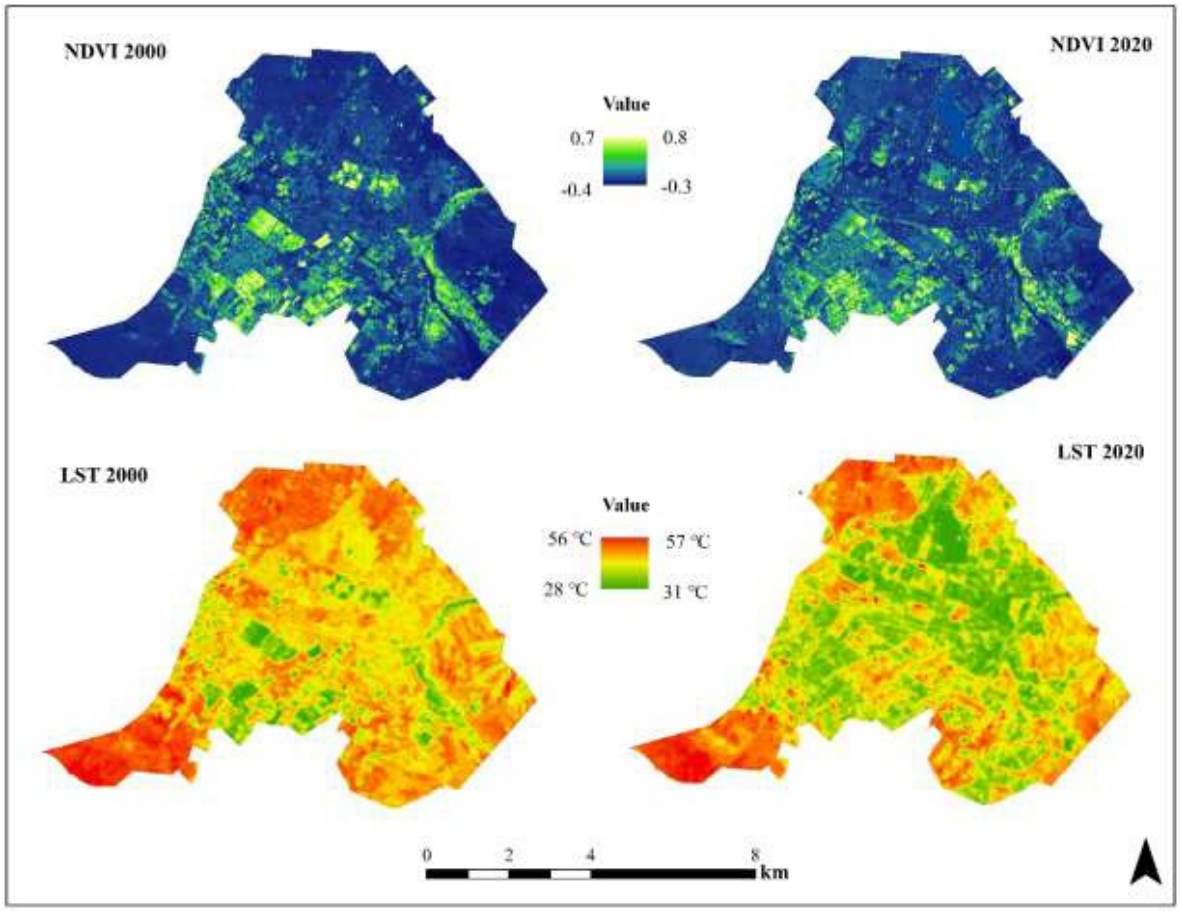

Fig. 3 NDVI and LST maps of 2000 and 2020

To extract the UGS, the diagnostic ROC test was used. Table. 3 represented the results of the test using several criteria of Youden index, AUC, Sensitivity, Specificity, Correct classification, and Misclassification. In terms of Youden index, sensitivity, and specificity criteria the diagnosis ability of NDVI in UGS identification was higher than LST performance in both years. In addition, the value of correct classification and misclassification confirms the better diagnosis performance of NDVI than LST in separating the UGS from non-UGS in both years.

Criteria	2000		2020	
	LST	NDVI	LST	NDVI
AUC	0.846	0.922	0.822	0.983
Significance level P (Area=0.5)	<0.0001	<0.0001	>0.0001	>0.0001
Youden index J	0.6067	0.8200	0.5975	0.9375
Correct classification	0.802	0.910	0.796	0.968
Misclassification	0.198	0.090	0.204	0.032
Sensitivity	0.74	0.877	0.902	0.988
Specificity	0.867	0.943	0.688	0.948
Associated threshold value	≤42.7638	>0.2009	≥41.87	<0.2683

Table 3 Youden's statistics for LST and NDVI (2000-2020)

Fig. 4 shows the ROC curves based on the sensitivity and specificity, identifying threshold values of ≤42.7 and ≤41° C for LST and 0.2< and 0.2683< for NDVI in 2000 and 2020, respectively. According to the area under curve (AUC) values, the performance of UGS extraction using LST was satisfactory in 2000 (0.846) and 2020 (0.822). The AUC using NDVI was classified as excellent in 2000 (0.922) and 2020 (0.983). Accordingly, UGSs were extracted using NDVI in both years as they exhibited a higher distinguishing performance (Fig. 5).

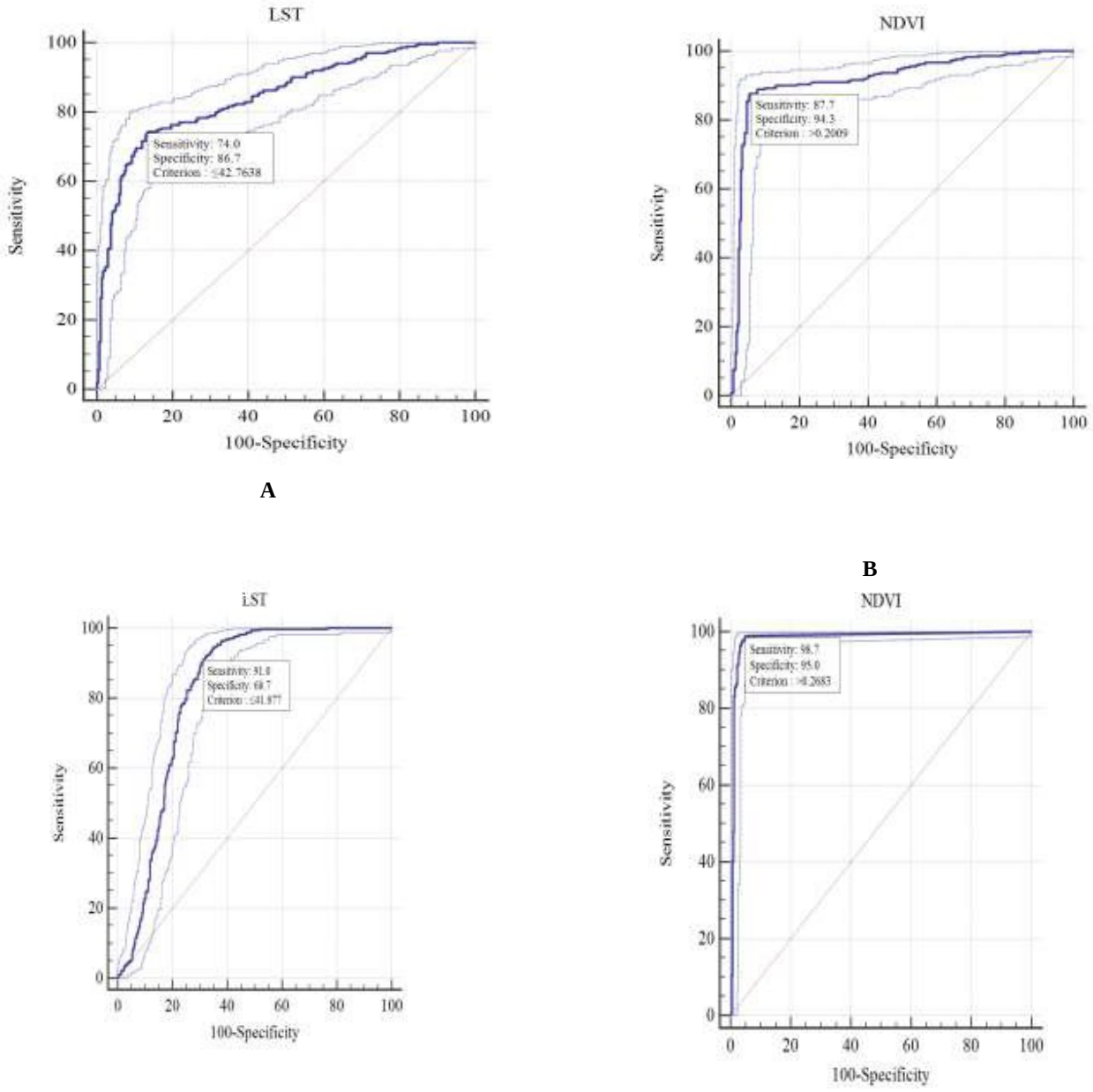

Fig. 4. AUC analysis: identifying the threshold value and their statistical accuracy to identify UGS versus non-UGS. A&B: AUC, sensitivity, specificity, and cut-off value for LST and NDVI in 2000, C& D: AUC, sensitivity, specificity, and cut-off value for LST and NDVI in 2020.

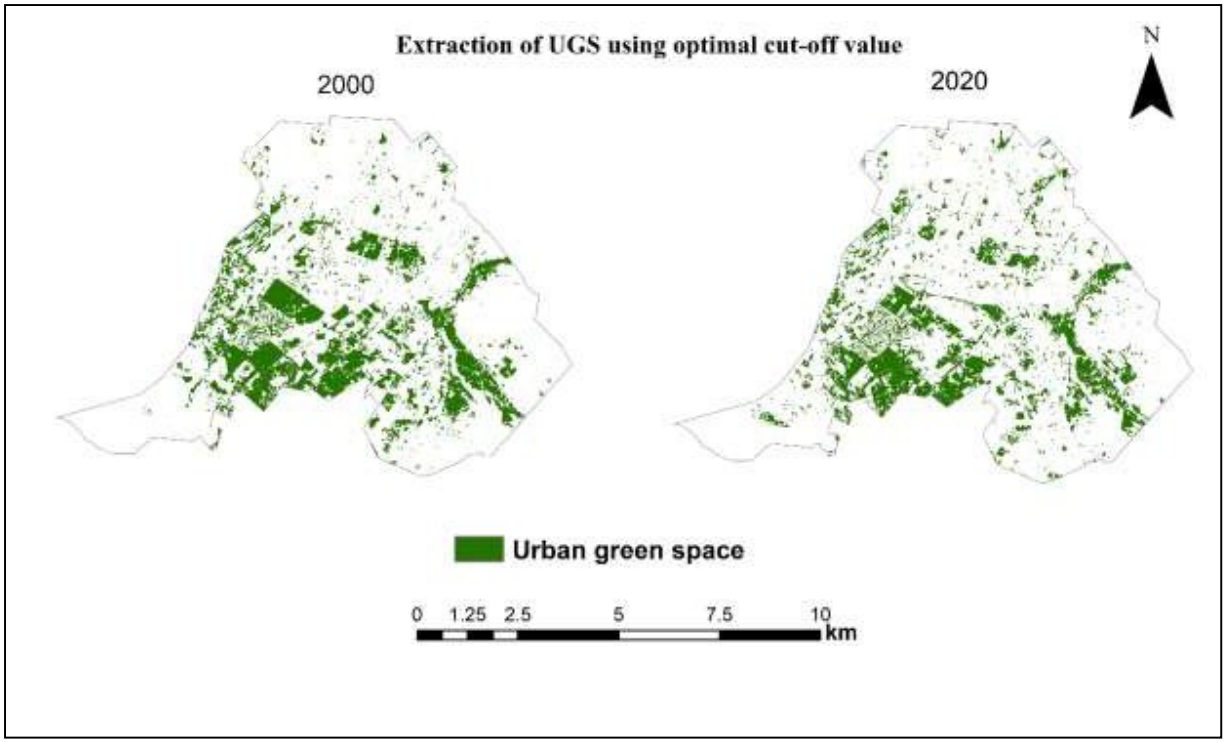

Fig. 5. UGS maps in 2000 and 2020

Fig. 5 shows the total area of UGS based on the NDVI threshold in 2000 and 2020, covering 48,000 and 41,000 hectares, respectively (decreased approximately by 20% over this time period).

3.2. Results of the Hot Spot Analysis

The output of Hot Spot analysis on the LST was a z-score map that was classified into four classes based on different confidence intervals of 99%, 95%, 90%, and not significant in 2000 and 2020 (Fig. 6). Then the z-score map was extracted by the UGS map and the output map was classified into four different classes. Table 4 represents cold green patches area in four classes in 2000 and 2020. Respectively 25% and 43% of the UGS in 2000 and 2020, mainly the farmlands and rangelands, were not significantly cold.

Table. 4 The area of UGS at different confidence levels in 2000 and 2020

Cold green patch at different confidence levels	2000 (ha)	2020 (ha)
99%	21,259	13,807
95%	11,502	6,413
90%	27,890	3,525
Not-significant	12,479.4	18,077.4

In order to achieve the highest accuracy in this research, we considered only the cold green patches (or GHS) at a 99% confidence level. In Fig. 6, the cold green patches or GHSs are shown at a 99% confidence level based on the z-score from the Hot Spot Analysis. According to this classification, the area of GHSs decreased by 35% over time.

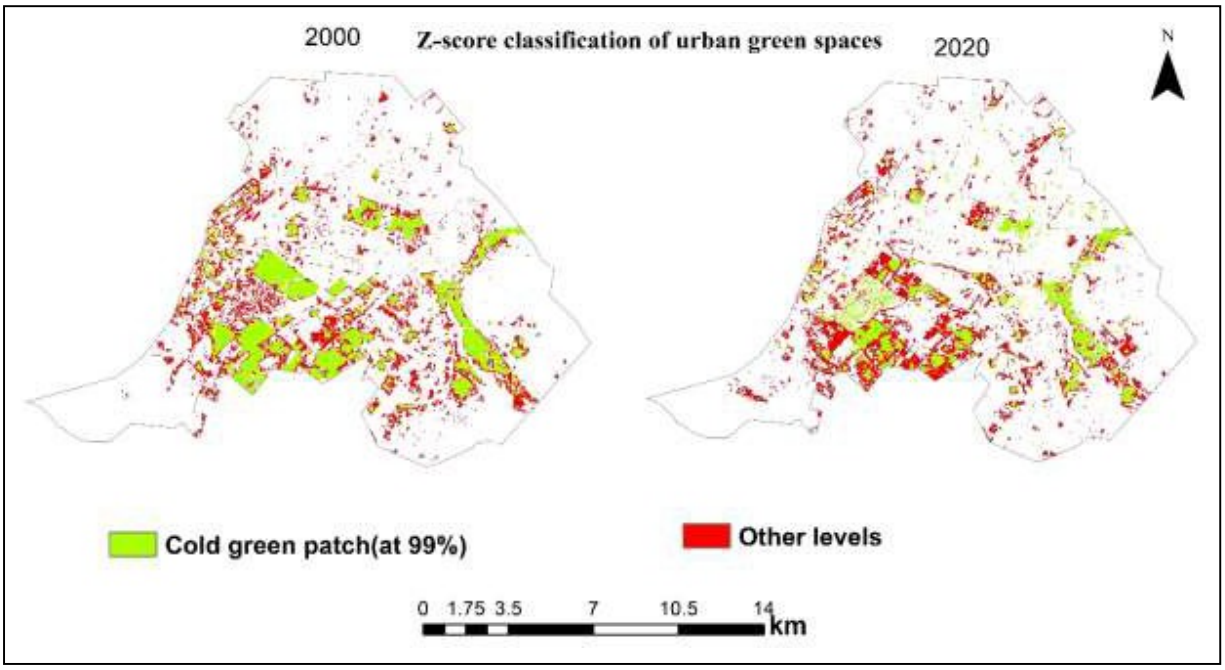

Fig. 6. UGS at a 99% (GHS) and other confidence levels

3.3. Result of Network-based analysis and pinch point identification

Using GHSs as nodes (Fig. 7 A& B) and the inverted NDVI maps as cost surfaces (Fig. 7 C& D), the distribution of the connectivity of the GHS current flow intensity map was produced using Circuitcape. 4 (Fig. 7 E& F).

The results of Circuitcape software was a current intensity map with different degrees of connectivity between GHSs (Fig. 7 E & F). Higher current values show stronger connections between GHSs. Subsequently, visually inspecting the current map and considering the pinch points definition, five main pinch points in the current map of 2020 were chosen as priority locations to increase the connectivity of GHS in the future (Fig 7. F). Observing the pinch points and land use map and google earth, in location 1, the barren land made a high cost to connectivity, while in points 2 and 4, the built-up area decreased the current intensity, and in points 3 and 5, the poor vegetation cover (i.e., rangeland and farmland) inhibited the linkage between GHS and decreased the current flow. In addition, in order to compare the current maps of two years, the pixel-based differentiation between the current maps of 2000 and 2020 was applied, illustrating the overall connectivity was higher in 2000 as compared to 2020. However, in the southern and eastern parts and a small area in the southeast of the city, the connectivity in 2020 was slightly higher than that of 2000 (Fig. 8).

3.4. Results of Patch-based analysis

The results of landscape metrics for GHS are represented in Table 5. The GHS occupied 11% and 7.2% of the total landscape in 2000 and 2020, respectively. The number of patches and the patch density increased from 2000 to 2020. While the LPI metric was lower in 2020 than in 2000; the large GHS converted to the small patches, and the LSI metric showed that the shape complexity increased during this time.

Table 5 Spatial attributes of the GHS in 2000 and 2020

Metric	2000	2020
PLAND	11	7.2
NP	222	458
PD	0.97	2.55
LPI	2.44	0.51
LSI	19.72	26.81

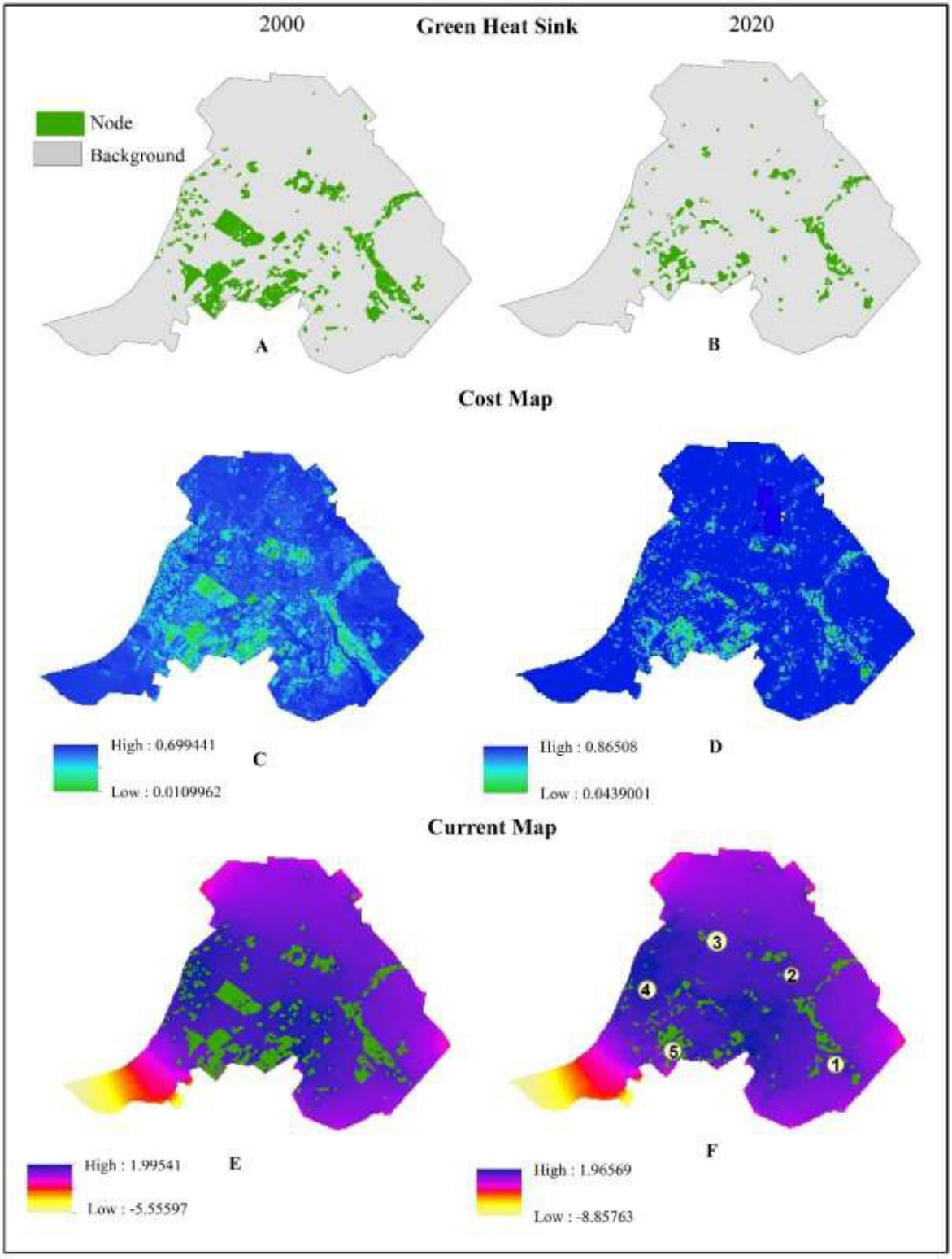

Fig. 7. Construction of network A&B: GHS as nodes in 2000 and 2020, C& D: Cost map of 2000 and 2020, and E & F: Distribution of current flow intensity in 2000 and 2020.

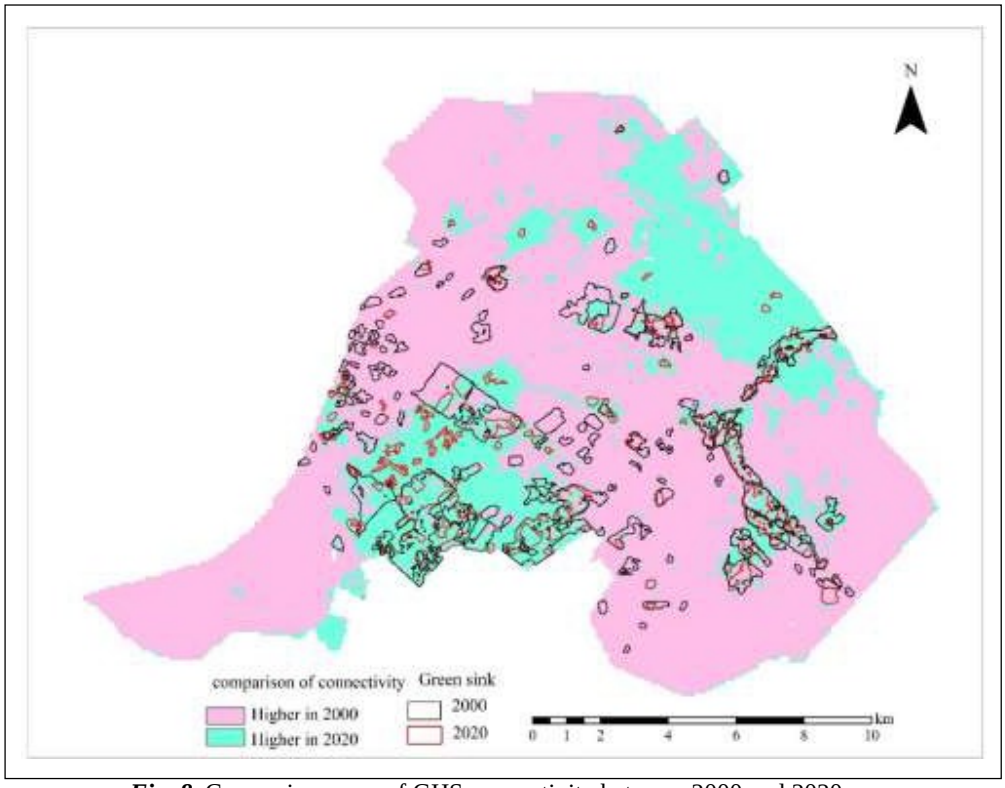

Fig. 8. Comparison map of GHS connectivity between 2000 and 2020

4. Discussion

The spatial pattern and connectivity of UGS are of importance in building a thermally comfortable urban landscape (Xie et al., 2015; Asgarian et al., 2015). In this research, over the past two decades, the LST pattern of the region has changed due to land use/land cover transformation. Green cover loss and urban expansion, together with lack or poor implementation of sustainable urban land use planning practices, resulted in both qualitative and quantitative degradation of green covers. It not only reduced the cooling performance of the urban landscape but also caused high-LST bare lands (thermal sources) to surround and further affect the thermal properties of built-up patches. Another substantial change in the LST pattern was seen in decreasing the temperature of the densely built-up area in 2020. Generally, this land use- LST pattern has been frequently observed in urban regions located in arid and semi-arid climatic zones like central Iran, where the diurnal surface UHI often does not form in the built-up area (the reasons for this phenomenon are beyond the scope of the research) (Haashemi et al., 2016; Azhdari et al., 2018; Madanian et al., 2018; Tayyebi et al., 2018).

NDVI-based optimal thresholding methods have been frequently utilized for land use and land cover classification (Doustfatemeh & Baleghi, 2016). However, in this research, we identified the threshold of NDVI and LST as two important variables of thermal landscape to extract the UGS. In terms of ecological studies, the diagnostic-ROC method has been often used to identify threshold values to evaluate the absence and presence of a species in habitats (Somodi et al., 2017; Piri Sahragard et al., 2018). Innovatively, in this study, we adopted this approach using LST and NDVI to diagnose the vegetation cover from non-vegetation cover in order to extract UGS. Applying this method, the statistical results indicated that NDVI outperformed LST in the extraction of UGS in both years. Because of the climatic attributes of the city (mentioned in the previous paragraph), the built-up area is almost cool and thermally is similar to green space; therefore, it makes a source of bias; subsequently, the LST variable cannot separate the UGS from the built-up area accurately. Therefore, it can be argued that in arid and semi-arid urban regions, the NDVI is a better variable than LST to extract the UGS.

The current research did not apply a common methodological approach to define thermal sink and source. In many studies, thermal sinks and sources were explained by land use classes (Pramanik & Punia, 2020), but in this research, the sinks (it was merely focused on the green heat sinks) were identified by Hot Spot analysis using the local statistic of Getis Ord Gi* at different confidence levels (considerably in the study, all the green patches were not classified as heat sinks due to poor vegetation cover in the warmest month of the year). This conclusion has been also supported in similar recent studies such as Tran et al. (2017), who emphasized that layer clustering by Getis Ord Gi* statistic is an effective approach to identify thermally-hot spots in urban environments.

The results indicated a significant GHS loss of 31% from 2000 to 2020, both through the complete disappearance of small patches and significant peripherical shrinkage of large GHSs. In comparison with UGS loss, results showed that around 14% of the remaining green spaces have lost their cooling performance in twenty years. Based on the

patch-level analysis, moreover, GHSs have become more fragmented such that the number and density of GHSs increased, whereas their size and shape became smaller and more complex. Inspecting land use maps and google earth images, during this time, many large garden patches have been fragmented to the sparse vegetation cover, rangeland, and bare land, which has not been significantly cold.

While most of the studies investigated patch-based composition and configuration attributes of UGS to maximize urban cooling capacity (Masoudi & Tan, 2019; Peng et al., 2016), Yu et al. (2021) emphasized that analyzing the overall connectivity from a network-based perspective can help identify critical locations that mitigate UHI (Yu et al., 2021). One of the main objectives of this research is to propose an approach to construct a network of UGS considering the temperature. In this way, the nodes included the cold green patches at a 99% confidence level and the cost map (i.e., numerically inverted NDVI) were inputs of network analysis using Circuit theory. The cost map means the lower the NDVI, the higher the resistance to connectivity and vice versa. Overall, NDVI served as a good classifier of GHSs (i.e., nodes) and also as an effective cost layer to investigate GHS connectivity. NDVI has been identified as the most explanatory factor of LST in arid and semi-arid zones of central Iranian landscapes with a combination of built-up, vegetation, and bare land components (Shafizadeh-Moghadam et al., 2020).

In the current research, the network-based analysis of GHSs indicated decreasing overall connectivity between GHSs over time. In dealing with the UHI network, Yu and colleagues proposed that green areas have the potential to break the UHI network in critical locations (i.e., pinch points) and decrease the urban temperature. Similarly, we identified pinch points as priority areas to enhance vegetation cover and, consequently, intensify the cooling effect within the city. As shown in Fig. 7, the five most important pinch points were distributed in different parts of the landscape, especially in areas where small-sized green patches were lost from 2000 through 2020. It can also be concluded that the designation of small green patches can play a significant part in constructing a better performing GHS network, while green cover conversion to bare lands may create a warmer urban landscape.

Theoretically, the structural connectivity of GHSs implies functional connectivity or functional potential such that the higher connectivity of GHS, the higher the cooling capacity of the landscape. Furthermore, from a theoretical point of view, in network-based analysis, the connectivity concept not only considers the nodes but also regards the resistance surface (B. H. McRae et al., 2008). It can be pretended that the linkage between the GHSs significantly depends on the matrix within a landscape. While the connectivity analysis from a patch-based approach (i.e., measuring the nearest neighbor metric) does not regard the resistance surface, so, it cannot represent the overall connectivity within the entire landscape (McRae et al., 2008; Yu et al., 2021).

Finally, based on the existing land cover in critical locations of the study area, we proposed three different implementations to enhance the GHS connectivity and improver UTE 1) green space can be established in existing vacant lots, 2) the density of vegetation can be improved in low-density green spaces by planting trees with a high shading effect and evapotranspiration, and 3) green walls and green roofs can be established in existing built-up areas.

In this study, several limitations should be acknowledged. First, due to the lack of experts' knowledge and accurate data, the study was restricted by only two NDVI and LST variables. For instance, in the case of benefitting from experts' knowledge related to the objective, a fuzzy approach (weighing different bio-physical factors) would link the structural connectivity (i.e., the connectedness of GHS) and functional connectivity (i.e., cooling capacity) in a more realistic and unbiased way (Pierik et al., 2016). The next limitation lies in setting up a cost map, we acknowledge that other physical and environmental factors can affect surface resistance. Therefore, layers of air temperature, wind flow direction, Normalized Differentiation Water Index (NDWI), albedo, or Digital Surface Model (DSM) can contribute to creating a cost map that has more conformity with the real environment. The connectivity analysis in future studies can be integrated with morphological spatial pattern analysis (MSPA), meaning that the GHSs can be classified into the core, bridge, islet, loop, edge, perforation, and bridge to explore the structural connectivity. Therefore, future research can address these limitations and apply them in different cities located in various climatic zones.

5. Conclusion

In an urban landscape, UGS connectivity is an essential spatial attribute that affects the urban thermal environment. In this research, we proposed a methodological framework to construct a network of the GHSs using circuit theory to examine the dynamic of overall GHS connectivity from a network-based and a patch-based analysis within Karaj city between 2000 and 2020. The results showed that the total area of UGS and GHS decreased in Karaj city. Based on the patch analysis, GHSs became highly fragmented, exhibiting smaller sizes, while the number of patches, patch density, and the complexity of the shape increased over the study period, particularly in the south and west parts of the city. The study's findings indicated that the overall connectivity decreased due to urbanization during the last two decades. In addition, based on the current flow intensity in 2020, several pinch points were recognized as priority locations to restore the connectivity of GHSs and consequently intensify the cooling effect. So that to improve the connectedness in these locations, the implementation of new green space, enhancing the current vegetation cover, and building of green roofs or green walls were proposed. Finally, we concluded that measuring the connectivity through the network-based analysis provides accurate information relating to the sink or source connection since it considers the resistance

surface or cost of the connectivity between the patches. Overall, this research offers an insight to the urban planner to optimize the spatial pattern of the UGS from the network-based perspective within an entire landscape toward urban temperature mitigation.

Declaration of interests

The authors declare that they have no known competing financial interests or personal relationships that could have appeared to influence the work reported in this paper.

References

Asgarian, A., Amiri, B. J., & Sakieh, Y. (2015). Assessing the effect of green cover spatial patterns on urban land surface temperature using the landscape metrics approach. *Urban Ecosystems*, *18*(1), 209-222.

Azhdari, A., Soltani, A., & Alidadi, M. (2018). Urban morphology and landscape structure effect on land surface temperature: Evidence from Shiraz, a semi-arid city. *Sustainable Cities and Society*, *41*, 853-864.

Bao, T., Li, X., Zhang, J., Zhang, Y., & Tian, S. (2016). Assessing the distribution of urban green spaces and its anisotropic cooling distance on urban heat island pattern in Baotou, China. *ISPRS International Journal of Geo-Information*, *5*(2), 12.

Bartesaghi-Koc, C., Osmond, P., & Peters, A. (2020). Quantifying the seasonal cooling capacity of 'green infrastructure types'(GITs): An approach to assess and mitigate surface urban heat island in Sydney, Australia. *Landscape and urban planning*, *203*, 103893.

Bastian, O., Haase, D., & Grunewald, K. (2012). Ecosystem properties, potentials and services–The EPPS conceptual framework and an urban application example. *Ecological indicators*, *21*, 7-16.

Bokaie, M., Zarkesh, M. K., Arasteh, P. D., & Hosseini, A. (2016). Assessment of urban heat island based on the relationship between land surface temperature and land use/land cover in Tehran. *Sustainable Cities and Society*, *23*, 94-104.

Calabrese, J. M., Fagan, W. F. J. F. i. E., & Environment, t. (2004). A comparison-shopper's guide to connectivity metrics. *2*(10), 529-536.

Caldas de Castro, M., & Singer, B. H. (2006). Controlling the false discovery rate: a new application to account for multiple and dependent tests in local statistics of spatial association. *Geographical analysis*, *38*(2), 180-208.

Chen, A., Zhao, X., Yao, L., & Chen, L. (2016). Application of a new integrated landscape index to predict potential urban heat islands. *Ecological Indicators*, *69*, 828-835.

Chen, L., Fu, B., & Zhao, W. (2008). Source-sink landscape theory and its ecological significance. *Frontiers of Biology in China*, *3*(2), 131-136.

Connors, J. P., Galletti, C. S., & Chow, W. T. (2013). Landscape configuration and urban heat island effects: assessing the relationship between landscape characteristics and land surface temperature in Phoenix, Arizona. *Landscape Ecology*, *28*(2), 271-283.

Cui, L., Wang, J., Sun, L., & Lv, C. (2020). Construction and optimization of green space ecological networks in urban fringe areas: A case study with the urban fringe area of Tongzhou district in Beijing. *Journal of Cleaner Production*, *276*, 124266.

Darvishi, A., Mobarghaee Dinan, N., Barghjelveh, S., & Yousefi, M. (2020). Assessment and Spatial Planning of Landscape Ecological Connectivity for Biodiversity Management (Case Study: Qazvin Province). *Iranian Journal of Applied Ecology*, *9*(1), 15-29.

da Silva, V. S., Salami, G., da Silva, M. I. O., Silva, E. A., Monteiro Junior, J. J., Alba, E. J. G., Ecology, & Landscapes. (2020). Methodological evaluation of vegetation indexes in land use and land cover (LULC) classification. *4*(2), 159-169.

Doustfatemeh, I., & Baleghi, Y. (2016). Comprehensive urban area extraction from multispectral medium spatial resolution remote-sensing imagery based on a novel structural feature. *International Journal of Remote Sensing*, *37*(18), 4225-4242.

Du, J., Xiang, X., Zhao, B., & Zhou, H. (2020). Impact of urban expansion on land surface temperature in Fuzhou, China using Landsat imagery. *Sustainable Cities and Society*, *61*, 102346.

Estoque, R. C., Murayama, Y., & Myint, S. W. (2017). Effects of landscape composition and pattern on land surface temperature: An urban heat island study in the megacities of Southeast Asia. *Science of the Total Environment*, *577*, 349-359.

Fawcett, T. (2006). An introduction to ROC analysis. *Pattern recognition letters*, *27*(8), 861-874.

Faraggi, D., & Reiser, B. (2002). Estimation of the area under the ROC curve. *Statistics in medicine*, *21*(20), 3093-3106.

Fluss, R., Faraggi, D., & Reiser, B. (2005). Estimation of the Youden Index and its associated cutoff point. *Biometrical Journal: Journal of Mathematical Methods in Biosciences*, *47*(4), 458-472.

Ghobadi, A., Khosravi, M., & Tavousi, T. (2018). Surveying of heat waves impact on the urban heat islands: Case study, the Karaj City in Iran. *Urban Climate*, *24*, 600-615.

Gillespie, T. W., Ostermann-Kelm, S., Dong, C., Willis, K. S., Okin, G. S., & MacDonald, G. M. (2018). Monitoring changes of NDVI in protected areas of southern California. *Ecological Indicators*, *88*, 485-494.

Grafius, D. R., Corstanje, R., Siriwardena, G. M., Plummer, K. E., & Harris, J. A. (2017). A bird's eye view: using circuit theory to study urban landscape connectivity for birds. *Landscape ecology*, *32*(9), 1771-1787.

Guo, S., Saito, K., Yin, W., & Su, C. (2018). Landscape connectivity as a tool in green space evaluation and optimization of the haidan district, beijing. *Sustainability*, *10*(6), 1979.

Halder, B., Bandyopadhyay, J., & Banik, P. (2021). Monitoring the effect of urban development on urban heat island based on remote sensing and geo-spatial approach in Kolkata and adjacent areas, India. *Sustainable Cities and Society*, *74*, 103186.

Haashemi, S., Weng, Q., Darvishi, A., & Alavipanah, S. K. (2016). Seasonal variations of the surface urban heat island in a semi-arid city. *Remote Sensing*, *8*(4), 352.

Hyseni, C., Heino, J., Bini, L. M., Bjelke, U., & Johansson, F. (2021). The importance of blue and green landscape connectivity for biodiversity in urban ponds. *Basic and Applied Ecology, 57*, 129-145.

Jamei, Y., Rajagopalan, P., & Sun, Q. C. (2019). Spatial structure of surface urban heat island and its relationship with vegetation and built-up areas in Melbourne, Australia. *Science of the Total Environment, 659*, 1335-1351.

Jana, M., & Sar, N. (2016). Modeling of hotspot detection using cluster outlier analysis and Getis-Ord Gi* statistic of educational development in upper-primary level, India. *Modeling Earth Systems and Environment, 2*(2), 60.

Karami, P., Rezaei, S., Shadloo, S., & Naderi, M. (2020). An evaluation of central Iran's protected areas under different climate change scenarios (A Case on Markazi and Hamedan provinces). *Journal of Mountain Science*, *17*(1), 68-82.

Koen, E. L., Bowman, J., Sadowski, C., & Walpole, A. A. (2014). Landscape connectivity for wildlife: development and validation of multispecies linkage maps. *Methods in Ecology and Evolution, 5*(7), 626-633.

Kong, F., Yin, H., Nakagoshi, N., & Zong, Y. (2010). Urban green space network development for biodiversity conservation: Identification based on graph theory and gravity modeling. *Landscape and urban planning, 95*(1-2), 16-27.

Kowe, P., Mutanga, O., Odindi, J., & Dube, T. (2021). Effect of landscape pattern and spatial configuration of vegetation patches on urban warming and cooling in Harare metropolitan city, Zimbabwe. *GIScience & Remote Sensing, 58*(2), 261-280.

Kwon, O. S., Kim, J. H., & Ra, J. H. (2021). Landscape Ecological Analysis of Green Network in Urban Area Using Circuit Theory and Least-Cost Path. *Land, 10*(8), 847.

Labrique, A. B., & Pan, W. K.-Y. (2010). Diagnostic tests: understanding results, assessing utility, and predicting performance. *American journal of ophthalmology, 149*(6), 878-881. e872.

Leitão, A. B., Miller, J., Ahern, J., & McGarigal, K. (2012). *Measuring landscapes: A planner's handbook*: Island press.

Li, W., Cao, Q., Lang, K., & Wu, J. (2017). Linking potential heat source and sink to urban heat island: Heterogeneous effects of landscape pattern on land surface temperature. *Science of the Total Environment, 586*, 457-465.

Lin, W., Yu, T., Chang, X., Wu, W., & Zhang, Y. (2015). Calculating cooling extents of green parks using remote sensing: Method and test. *Landscape and Urban Planning, 134*, 66-75.

Liu, Z., He, C., & Wu, J. (2016). The relationship between habitat loss and fragmentation during urbanization: an empirical evaluation from 16 world cities. *PLoS One, 11*(4), e0154613.

Liu, Y., Huang, T.-T., & Zheng, X. J. U. E. (2022). A method of linking functional and structural connectivity analysis in urban green infrastructure network construction. 1-17.

Lookingbill, T. R., & Minor, E. S. (2017). Assessing multi-scale landscape connectivity using network analysis. In *Learning Landscape Ecology* (pp. 193-209): Springer.

Madanian, M., Soffianian, A. R., Koupai, S. S., Pourmanafi, S., Momeni, M. J. S. c., & society. (2018). The study of thermal pattern changes using Landsat-derived land surface temperature in the central part of Isfahan province. *39*, 650-661.

Maimaitiyiming, M., Ghulam, A., Tiyip, T., Pla, F., Latorre-Carmona, P., Halik, Ü., . . . Caetano, M. (2014). Effects of green space spatial pattern on land surface temperature: Implications for sustainable urban planning and climate change adaptation. *ISPRS Journal of Photogrammetry and Remote Sensing, 89*, 59-66.

Marulli, J., & Mallarach, J. M. (2005). A GIS methodology for assessing ecological connectivity: application to the Barcelona Metropolitan Area. *Landscape and urban planning, 71*(2-4), 243- 262.

Masoudi, M., & Tan, P. Y. (2019). Multi-year comparison of the effects of spatial pattern of urban green spaces on urban land surface temperature. *Landscape and urban planning, 184*, 44-58.

Masoudi, M., Tan, P. Y., & Fadaei, M. (2021). The effects of land use on spatial pattern of urban green spaces and their cooling ability. *Urban climate, 35*, 100743.

McGarigal, K., & Marks, B. J. (1995). Spatial pattern analysis program for quantifying landscape structure. *Gen. Tech. Rep. PNW-GTR-351. US Department of Agriculture, Forest Service, Pacific Northwest Research Station*, 1-122.

McRae, B. H., Dickson, B. G., Keitt, T. H., & Shah, V. B. (2008). Using circuit theory to model connectivity in ecology, evolution, and conservation. *Ecology, 89*(10), 2712-2724.

Mokhtari, Z., Barghjelveh, S., & Sayahnia, R. (2021). Heterogeneity of the thermal environment and its ecological evaluation in the urban region of Karaj. *Geography and Environmental Sustainability, 11*(4), 37-58.

Pelletier, D., Clark, M., Anderson, M. G., Rayfield, B., Wulder, M. A., & Cardille, J. A. (2014). Applying circuit theory for corridor expansion and management at regional scales: tiling, pinch points, and omnidirectional connectivity. *PLoS One, 9*(1), e84135.

Peng, J., Xie, P., Liu, Y., & Ma, J. (2016). Urban thermal environment dynamics and associated landscape pattern factors: A case study in the Beijing metropolitan region. *Remote sensing of environment, 173*, 145-155.

Pierik, M. E., Dell'Acqua, M., Confalonieri, R., Bocchi, S., & Gomarasca, S. (2016). Designing ecological corridors in a fragmented landscape: A fuzzy approach to circuit connectivity analysis. *Ecological indicators, 67*, 807-820.

Piri Sahragard, H., Ajorlo, M., & Karami, P. (2018). Modeling habitat suitability of range plant species using random forest method in arid mountainous rangelands. *Journal of Mountain Science, 15*(10), 2159-2171.

Pramanik, S., & Punia, M. (2020). Land use/land cover change and surface urban heat island intensity: source–sink landscape-based study in Delhi, India. *Environment, Development and Sustainability, 22*(8), 7331-7356.

Qin, Z., Karnieli, A., & Berliner, P. (2001). A mono-window algorithm for retrieving land surface temperature from Landsat TM data and its application to the Israel-Egypt border region. *International journal of remote sensing, 22*(18), 3719-3746.

Qureshi, S., Haase, D., & Coles, R. (2014). The theorized urban gradient (TUG) method—a conceptual framework for socio-ecological sampling in complex urban agglomerations. *Ecological Indicators, 36*, 100-110.

Reis, C., & Lopes, A. (2019). Evaluating the cooling potential of urban green spaces to tackle urban climate change in Lisbon. *Sustainability, 11*(9), 2480.

Saaroni, H., Amorim, J. H., Hiemstra, J., & Pearlmutter, D. (2018). Urban Green Infrastructure as a tool for urban heat mitigation: Survey of research methodologies and findings across different climatic regions. *Urban climate, 24*, 94-110.

Shafizadeh-Moghadam, H., Weng, Q., Liu, H., & Valavi, R. (2020). Modeling the spatial variation of urban land surface temperature in relation to environmental and anthropogenic factors: a case study of Tehran, Iran. *GIScience & Remote Sensing*, *57*(4), 483-496.

Shih, W. J. H. I. (2017). Greenspace patterns and the mitigation of land surface temperature in Taipei metropolis. *60*, 69-80.

Somodi, I., Lepesi, N., & Botta-Dukát, Z. (2017). Prevalence dependence in model goodness measures with special emphasis on true skill statistics. *Ecology and Evolution*, *7*(3), 863-872.

Songchitruksa, P., & Zeng, X. (2010). Getis–Ord spatial statistics to identify hot spots by using incident management data. *Transportation research record*, *2165*(1), 42-51.

Sun, R., Xie, W., & Chen, L. (2018). A landscape connectivity model to quantify contributions of heat sources and sinks in urban regions. *Landscape and urban planning*, *178*, 43-50.

Taleshi, M., & Ghobadi, A. (2012). Urban land use sustainability assessment through evaluation of compatibility matrix case study: Karaj City. *OIDA International Journal of Sustainable Development*, *3*(1), 57-64.

Taylor, L., & Hochuli, D. F. (2017). Defining greenspace: Multiple uses across multiple disciplines. *Landscape and urban planning*, *158*, 25-38.

Taylor, P. D., Fahrig, L., Henein, K., & Merriam, G. (1993). Connectivity is a vital element of landscape structure. *Oikos*, 571-573.

Tayyebi, A., Shafizadeh-Moghadam, H., & Tayyebi, A. H. (2018). Analyzing long-term spatio-temporal patterns of land surface temperature in response to rapid urbanization in the mega-city of Tehran. *Land Use Policy*, *71*, 459-469.

Tran, D. X., Pla, F., Latorre-Carmona, P., Myint, S. W., Caetano, M., & Kieu, H. V. (2017). Characterizing the relationship between land use land cover change and land surface temperature. *ISPRS Journal of Photogrammetry and Remote Sensing*, *124*, 119-132.

Turner, M. G. J. A. r. o. e., & systematics. (1989). Landscape ecology: the effect of pattern on process. *20*(1), 171-197.

Uy, P. D., & Nakagoshi, N. (2007). Analyzing urban green space pattern and eco-network in Hanoi, Vietnam. *Landscape and Ecological Engineering*, *3*(2), 143-157.

Voogt, J. A., & Oke, T. R. (2003). Thermal remote sensing of urban climates. *Remote sensing of environment*, *86*(3), 370-384.

Wang, F., Qin, Z., Song, C., Tu, L., Karnieli, A., & Zhao, S. (2015). An improved mono-window algorithm for land surface temperature retrieval from Landsat 8 thermal infrared sensor data. *Remote Sensing*, *7*(4), 4268-4289.

Weng, Q. (2009). Thermal infrared remote sensing for urban climate and environmental studies: Methods, applications, and trends. *ISPRS Journal of Photogrammetry and Remote Sensing*, *64*(4), 335-344.

Wong, H. B., & Lim, G. H. (2011). Measures of diagnostic accuracy: sensitivity, specificity, PPV and NPV. *Proceedings of Singapore healthcare*, *20*(4), 316-318.

Xie, M., Gao, Y., Cao, Y., Breuste, J., Fu, M., & Tong, D. (2015). Dynamics and temperature regulation function of urban green connectivity. *Journal of Urban Planning and Development*, *141*(3), A5014008.

Xu, L., You, H., Li, D., & Yu, K. (2016). Urban green spaces, their spatial pattern, and ecosystem service value: The case of Beijing. *Habitat International*, *56*, 84-95.

Yengoh, G. T., Dent, D., Olsson, L., Tengberg, A. E., & Tucker III, C. J. (2015). *Use of the Normalized Difference Vegetation Index (NDVI) to assess Land degradation at multiple scales: current status, future trends, and practical considerations*: Springer.

Yu, Z., Zhang, J., & Yang, G. (2021). How to build a heat network to alleviate surface heat island effect? *Sustainable Cities and Society*, *74*, 103135.

Zardo, L., Geneletti, D., Pérez-Soba, M., & Van Eupen, M. (2017). Estimating the cooling capacity of green infrastructures to support urban planning. *Ecosystem services*, *26*, 225-235.

Zhang, Z., Meerow, S., Newell, J. P., & Lindquist, M. (2019). Enhancing landscape connectivity through multifunctional green infrastructure corridor modeling and design. *Urban forestry & urban greening*, *38*, 305-317.

Zhao, H., Zhang, H., Miao, C., Ye, X., & Min, M. (2018). Linking heat source–sink landscape patterns with analysis of urban heat islands: Study on the fast-growing Zhengzhou City in Central China. *Remote Sensing*, *10*(8), 1268.

Zhibin, R., Haifeng, Z., Xingyuan, H., Dan, Z., & Xingyang, Y. (2015). Estimation of the relationship between urban vegetation configuration and land surface temperature with remote sensing. *Journal of the Indian Society of Remote Sensing*, *43*(1), 89-100.

Zhou, X., & WANG, Y. C. (2011). Dynamics of land surface temperature in response to land-use/cover change. *Geographical Research*, *49*(1), 23-36.